JOURNAL OF MATERIALS SCIENCE **35** (2000) 3097–3103

The influence of matrix on the quantum size effect of CdSe microcrystals-doped thin films

H. NASU*, T. IWANO, T. HASHIMOTO, K. KAMIYA
Department of Chemistry for Materials, Faculty of Engineering, Mie University, Kamihama, Tsu 514-8507, Japan
E-mail: nasu@chem.mie-u.ac.jp

CdSe microcrystals were successfully dispersed in GeO_2 glass and CaF_2 crystal thin films by rf-sputtering. All films prepared showed the blue shift of absorption edge in visible spectra due to quantum size effect. The amount of the blue shift of the films increased with decreasing the size of the microcrystals. Comparing the amount of the particle size–depending blue shift of CdSe microcrystals dispersed in between the GeO_2, CaF_2 and SiO_2 matricies, the influence of the matrix on the shift was found. Therefore, it can be said that there is an influence of the matrix on the quantum size effect. From the modified theoretical calculation, the influence of matrix was considered to appear through Coulomb interaction between electrons and holes.

1. Introduction

Since Jain and Lind first reported high potential of the semiconductor-doped glasses as photonic device owing to their large third-order optical nonlinearity [1], extensive studies have been carried out for the optical properties and/or the quantum size effect of semiconductor-doped glass systems [2–14]. In these aggressive works, the magnitude of $\chi^{(3)}$ to in the order of 10^{-6} esu has been attained and the relaxation time has been reduced to in some tens ps. At the same time, it has been revealed that various kinds of semiconductor can be used as dopants for the glass, crystal or polymer matrix. For instance, CuBr, CuCl, CdS, CdSe, CdTe, ZnSe, PbS, Si and Ge microcrystals were successfully incorporated in the various matricies, and the quantum size effect and opitcal nonlinearity were examined [2–14].

The quantum size effect is theoretically classified into two types. One is exciton confinement effect and the other is the independent confinement effect of electron and hole. When the radius of the microcrystal is sufficiently larger than the exciton Bohr radius, the exciton confinement effect should occur. On the other hand, when the radius is comparable or smaller than the exciton Bohr radius, the independent confinement of electrons and holes should take place [9]. As previously reported [15], the semiconductors with small exciton Bohr radius such as CuCl or CuBr follow the exciton confinement, and the matrix affects should only the ditribution of the semiconductor particle size [15]. On the other hand, CdSe microcrystals or quantum dotts should follow the independent confinement rule. However, the significant deviation from the independent confinement was found in the CdSe-doped SiO_2 glass film [9]. It is considered that this deviation is caused by the Coulomb interaction between electrons and holes, which should be also influenced by matrix. However, there has been no systematic works on the influence of the matrix on the quantum size effect in the semiconductor-doped glasses. Thus, this paper deals with the CdSe microcrystal-doped GeO_2 and CaF_2 thin films to explore the influence of the matrix on the quantum size effect.

2. Experimental procedure

Magnetron rf-sputtering method was used to prepare CdSe microcrystals-doped thin films. For CdSe-doped GeO_2 glass thin films, the crushed melt-quenched GeO_2 glass powders were homogeneously scattered on the target plate, and CdSe pellets were put on the powders. The relative surface area ratio of CdSe to GeO_2 was varied from 17.2 to 28.6%. Substrates used were SiO_2 glass for optical measurements, offset Si for X-ray diffraction and KBr for TEM (transmission electron microscopy). Sputtering power was varied from 80 W to 150 W, substrate temperature from 160°C to 320°C.

Similarly, CdSe-doped CaF_2 thin films were prepared using the magnetron sputtering equipment. The CaF_2 powders were homogeneously scattered on the target, and CdSe pellets were placed on the powders. The relative surface area ratio of CdSe was varied from 9.5% to 25.6%, the input power was in the range from 60 W to 90 W and subatrate temperature was kept at 160°C. The different kinds of substrates described above were used for the respective purposes.

X-ray diffraction (XRD) patterns of the films were measured to explore the crystal phases with Shimadzu XD-610X diffractometer using Ni filtered Cu K_α radiation as a source. X-ray phtoelectron spectroscopy (XPS) (Shimadzu ESCA 750 and ESCA PAC 760) was used to

* Author to whom all correspondence should be addressed.

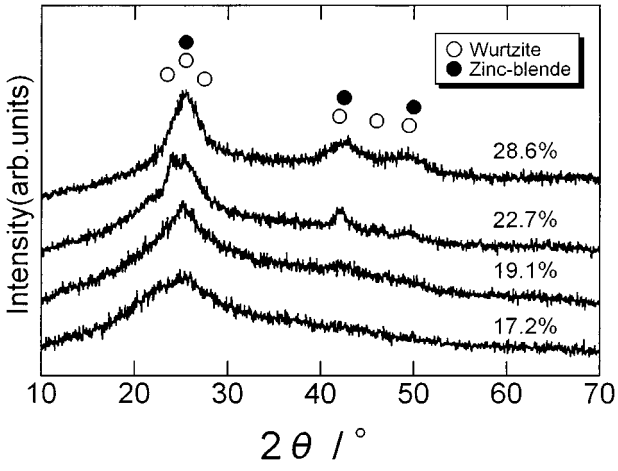

Figure 1 XRD patterns of CdSe-doped GeO_2 glass thin films prepared using various relative surface area ratio.

investigate the chemical bonding state and concentration of each element in the films. Mg K_α line was used as an X-ray source and the binding energy was caliblated against C 1s peak. Visible spectra were obtained by Shimadzu UV-VIS-NIR Recording Spectrometer at room temperature. The shape and size of the microcrystals were explored using transmission electron microscope (TEM) (Hitachi H-800).

3. Results

3.1. CdSe-doped GeO_2 glass thin films

Fig. 1 shows XRD patterns of the films sputtered using various surface area ratios under the applied voltage of 150 W at the substrate temperature of 160°C. Two types of CdSe crystals having wurtzite and zinc-blende structures are seen in all the patterns. The diffraction lines become sharper with increasing surface area ratio, and thus one can point out the mean particle size of microcrystal increasing with increasing the ratio. This is the same tendency as in the CdSe-doped silica films [9]. With respect to substrate temperature, the most sharp diffraction peak was obtained at 270°C, and the broadening of the peak occurred at higher substrate temperature. This fact means that there is an appropriate temperature to increase the particle size. As for input power, there is no obvious difference in XRD patterens between the films sputtered under 100 W and 150 W.

Fig. 2a and b depict typical XPS spectra of $Cd3d_{5/2}$ and Se 3d of a film, respectively. Spectra of Cd snd Se are seen to correspond with those in CdSe, implying that only CdSe is formed in the films and oxidization of incorporated CdSe scarecely occurs. And, no GeSe nor Ge formation is detected from Ge 3d spectra, and the peak position agrees with that of GeO_2. Thus, it can be said that CdSe is successfully doped in GeO_2 glass thin films.

A typical TEM picture of the CdSe-doped GeO_2 glass thin film is shown in Fig. 3. One can see that dark spots are scattered in the films. The dark spots correspond to CdSe microcrystals. Basically, CdSe microcrystals are homogeneously scattered in the film. The shape of particles looks sphere.

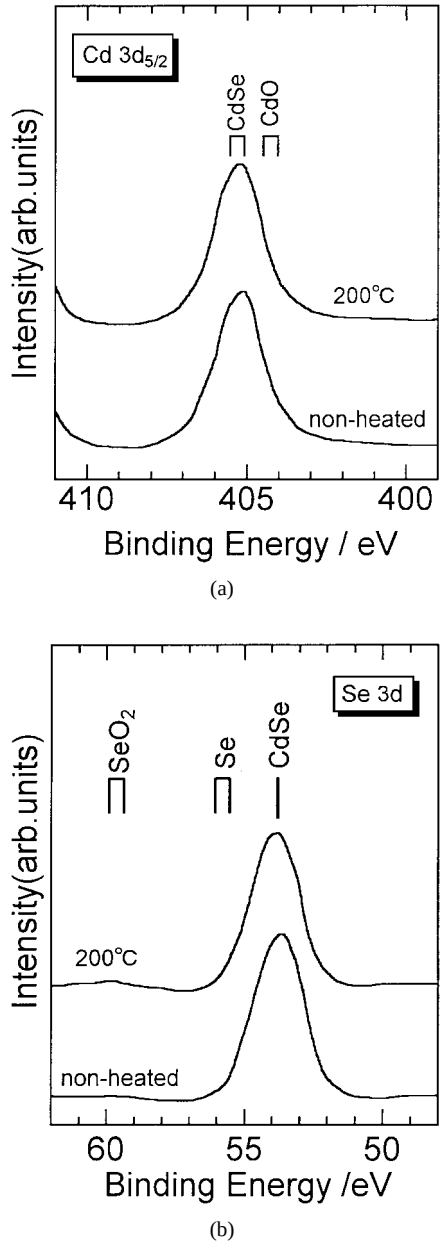

Figure 2 XPS spectra of (a) Cd $3d_{5/2}$ and (b) Se 3d in CdSe-doped GeO_2 glass thin films.

The absorption spectra are shown in Fig.4. The absorption edge shifts to shorter wavelength as the relative surface area ratio CdSe to GeO_2 at preparation decreases, which indicates the existense of the quantum size effect since the particle size decreases as the ratio decreases.

3.2. CdSe-doped CaF_2 thin films

Fig. 5 shows XRD patterns of CdSe-doped CaF_2 films prepared at various relative surface area ratios. Besides the diffraction peaks of CaF_2 crystalline matrix, the peaks of CdSe comes to be intense as the surface area ratio increases. This means that the mean particle radius of incorporated CdSe increases as the ratio increases like in CdSe-doped GeO_2 or SiO_2 glass thin films. The crystal types seen are zinc-blende and wurzite type ones.

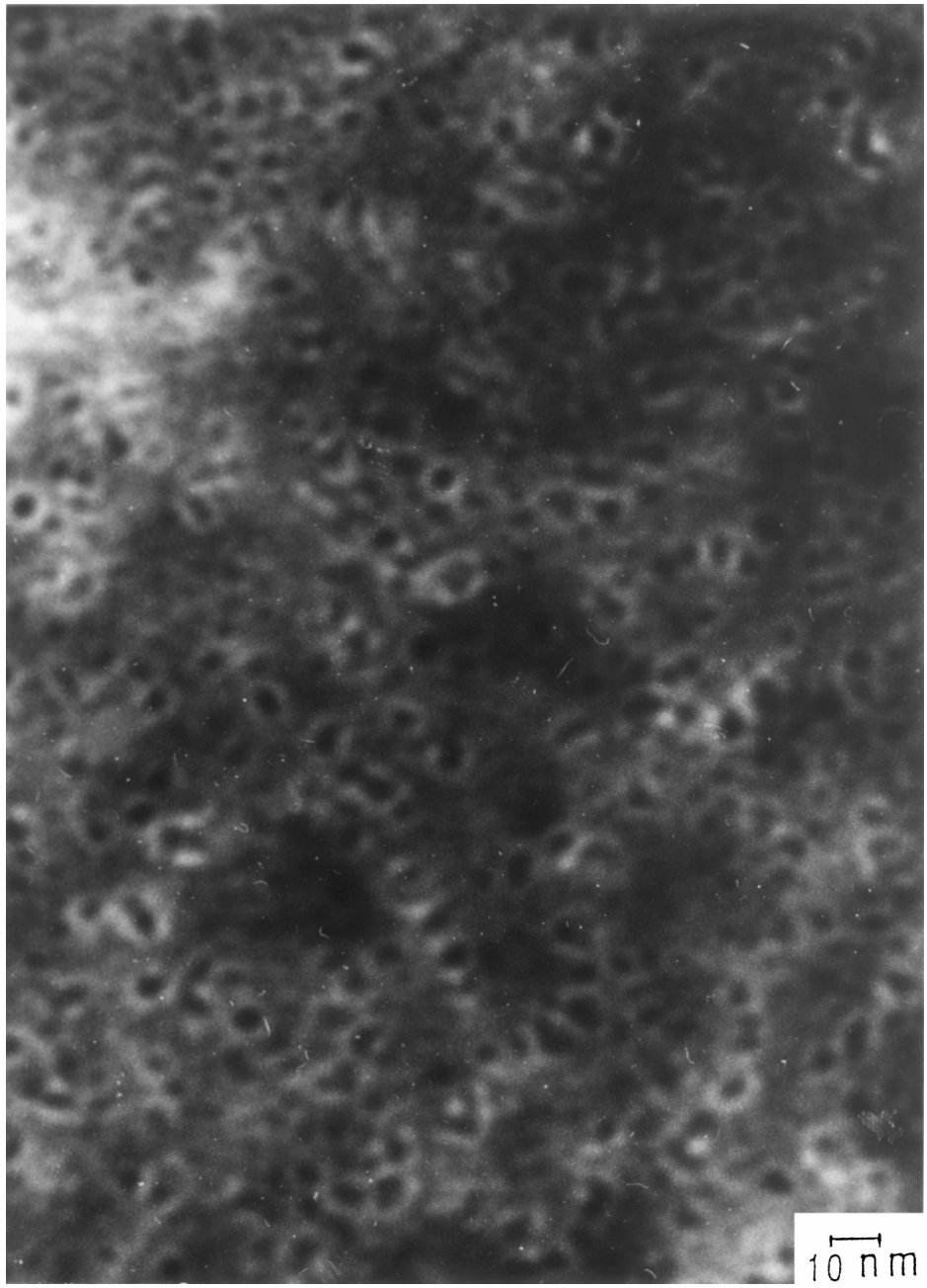

Figure 3 A TEM picture of CdSe-doped GeO_2 glass thin films (×600,000).

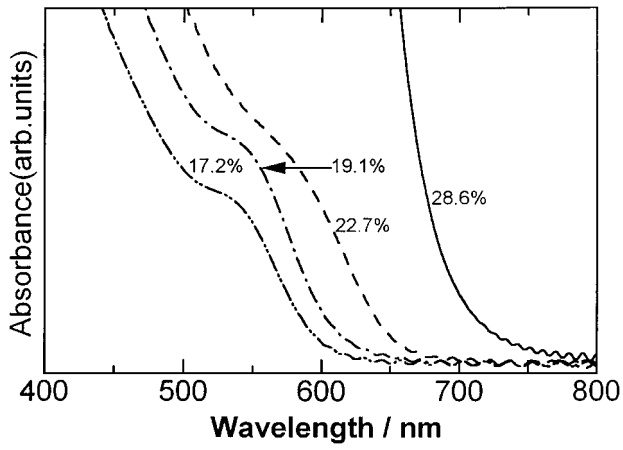

Figure 4 The absorption spectra of CdSe-doped GeO_2 glass thin films.

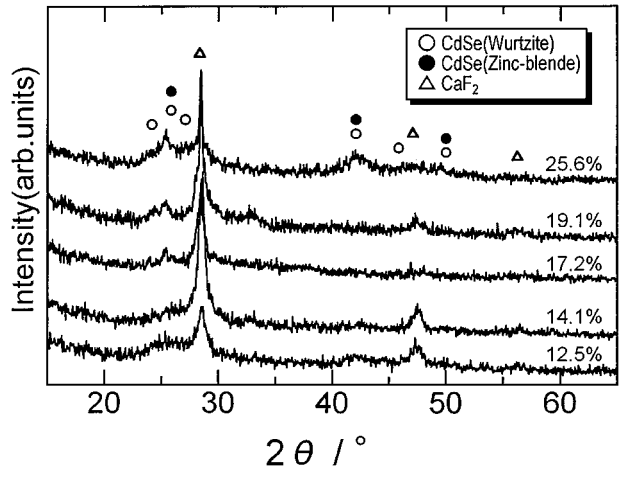

Figure 5 XRD patterns of CdSe-doped CaF_2 crystal thin films prepared using various relative surface area ratio.

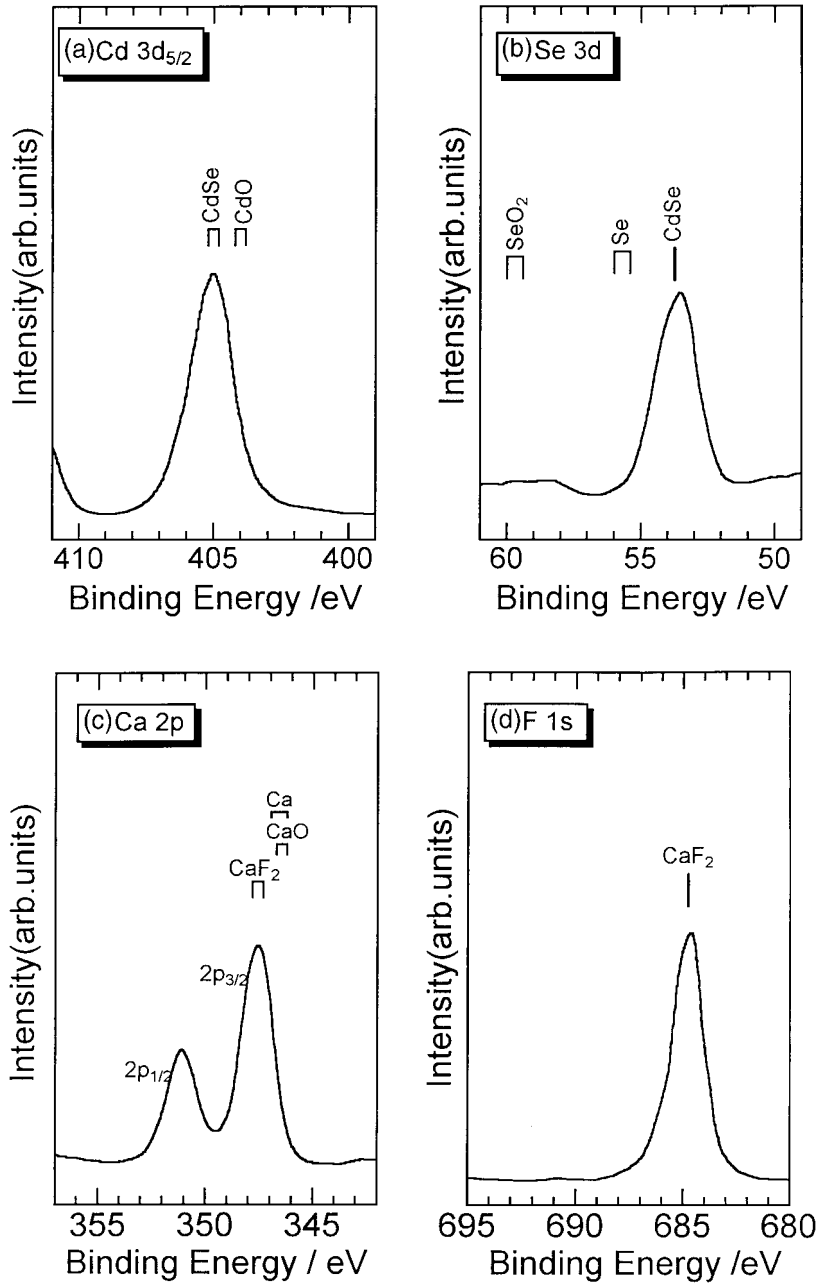

Figure 6 XPS spectra of (a)Cd $3d_{5/2}$, (b)Se 3d, (c) Ca 2p and (d) F1s in CdSe-doped CaF_2 crystal thin films.

XPS spectra of the films are shown in Fig. 6a–d for Cd $3d_{5/2}$, Se 3d, Ca 2p and F1s, respectively. From the figures, it is pointed out that Cd and Se exist as CdSe without any oxidization, and that Ca and F exist as CaF_2 in the films. No oxidization or reducion of chemical species is detected.

In TEM picture depicted in Fig.7, black spots are seen in the obscure background. The shape of the spots look circular. Then the deposited particles seem to be spherical. From the figure, it can be noted that the microcrystals are not formed at the grain boundary of CaF_2 but included in the matrix crystals.

With respect to absorption spectra in Fig. 8, the absorption edge shifts to shorter wavelength with decreasing relative surface area ratio as in the CdSe-doped GeO_2 glass thin films, in other words, with decreasing microcrystal size. It means the occurrence of quantum size effect in the film.

4. Discussion

As described in the section of the introduction, the quantum size effect is theoretically divided into two categories. On the basis of the theory, the quantum size effect of CdSe-doped should follow electron-hole independent confinement rule since the Bohr radius of the exciton of CdSe is sufficiently larger than the microcrystal size. Theoretically, the amount of blue shift (Δ Eg) as a function of microcrystal radius (R) should satisfy the following equations [9],

$$\Delta \mathrm{Eg} = \frac{h^2}{2\mu}\left(\frac{\pi}{R}\right)^2 \tag{1}$$

$$\frac{1}{\mu} = \frac{1}{m_\mathrm{e}} + \frac{1}{m_\mathrm{h}} \tag{2}$$

where μ is, so-called, reduced mass, m_e and m_h are the effective mass of electron and hole, respectively.

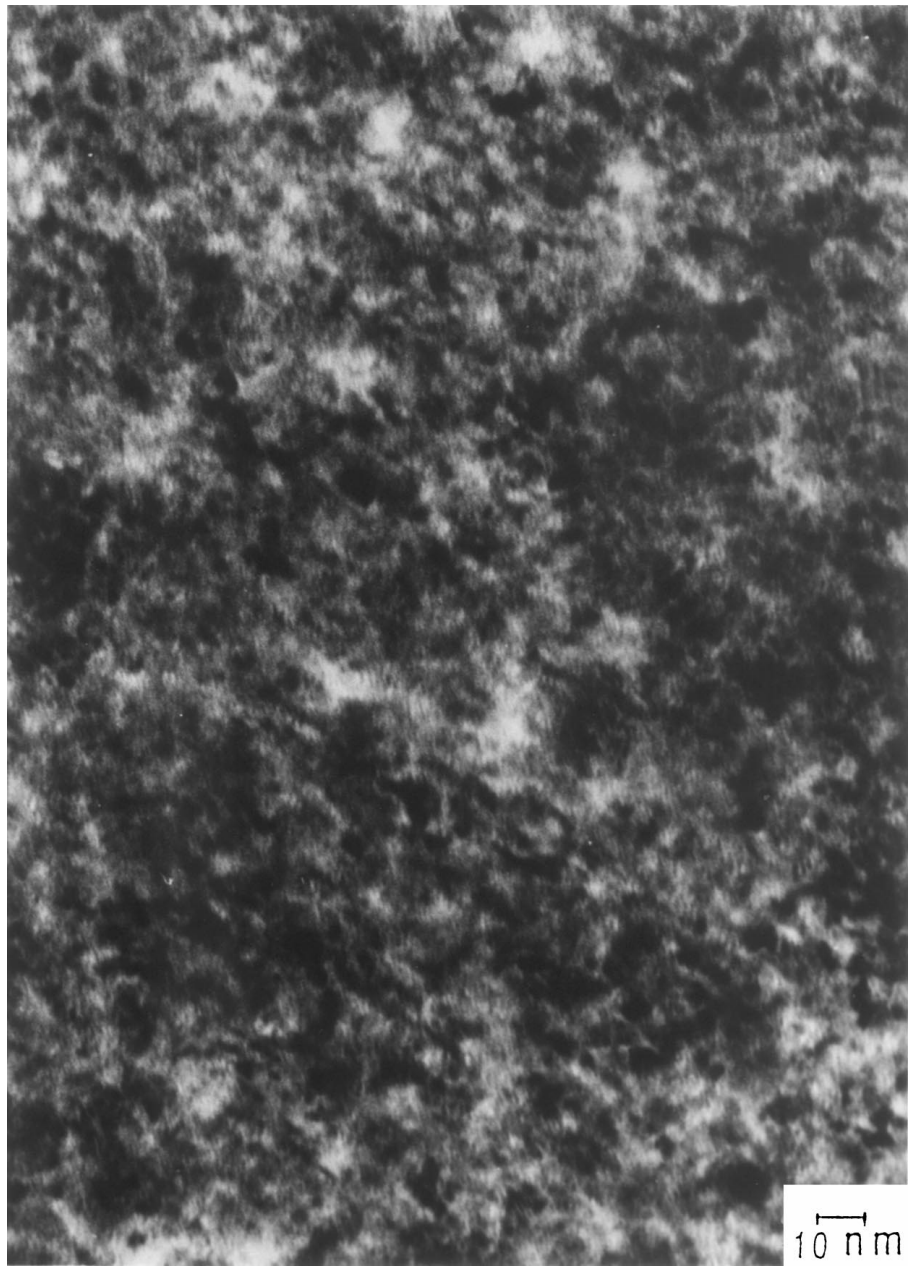

Figure 7 A TEM picture of CdSe-doped CaF_2 crystal thin films (×600,000).

In ref. [9], the experimental relation between ΔEg and R significantly deviated from Equation 1 in the CdSe-doped silica glass thin films. Thus, in order to explain this deviation, Coulomb interaction between electrons and holes and the squeezed exciton effect were taken into account [9] as

$$\Delta \mathrm{Eg} = \frac{h^2}{2\mu}\left(\frac{\pi}{R}\right)^2 - 1.786\frac{e^2}{\varepsilon R} - 0.248\mathrm{Ry}^* \qquad (3)$$

where ε is dielectric constant, Ry^* is effective Rydberg constant. In addition to Equation 3, the variation of ε depending on particle size has been taken into consideration by Haken potential [16],

$$\frac{1}{\varepsilon(R^*)} = \frac{1}{\varepsilon_\infty} - \left(\frac{1}{\varepsilon_\infty} - \frac{1}{\varepsilon_0}\right) \times \left(1 - \frac{\exp(-R^*/\rho_1) + \exp(-R^*/\rho_2)}{2}\right) \qquad (4)$$

where ε_∞ and ε_0 are the dielectric constant at frequency infinite and zero, respectively, R^* is the mean distance of electron and hole and ρ_1 and ρ_2 are the polaron radius of electron and hole, respectively.

On the other hand, when exciton confinement takes place, the ΔEg is expressed as

$$\Delta \mathrm{Eg} = \frac{h^2}{2M}\left(\frac{\pi}{R}\right)^2 \qquad (5)$$

where $M = m_\mathrm{e} + m_\mathrm{h}$, and called translational mass.

Fig. 9 shows the amount of the blue shift, Δ Eg, of CdSe-doped GeO_2 glass thin films as a function of reciprocal microcrystal radius. As has been seen in CdSe-doped SiO_2 glass thin films, the experimental plots significantly deviate from both the theoretical curves given by of Equations 1 and 5. The experimental plots according to Equation 3 are shown in Fig. 10. Two curves of the theoretical plots of Equation 3 using ε of CdSe and GeO_2 are also shown for comparison. As seen in

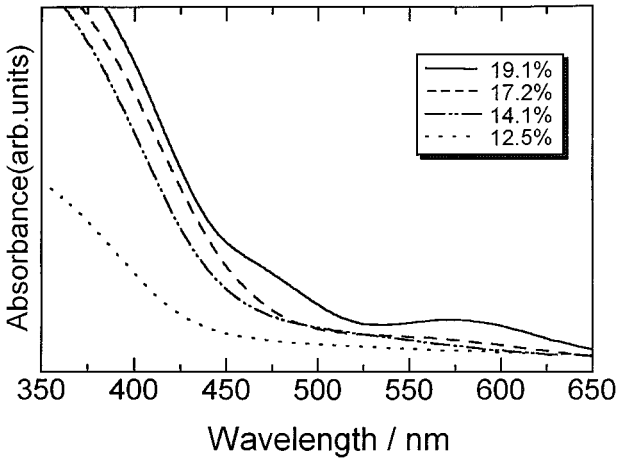

Figure 8 The absorption spectra of CdSe-doped CaF_2 crystal thin films.

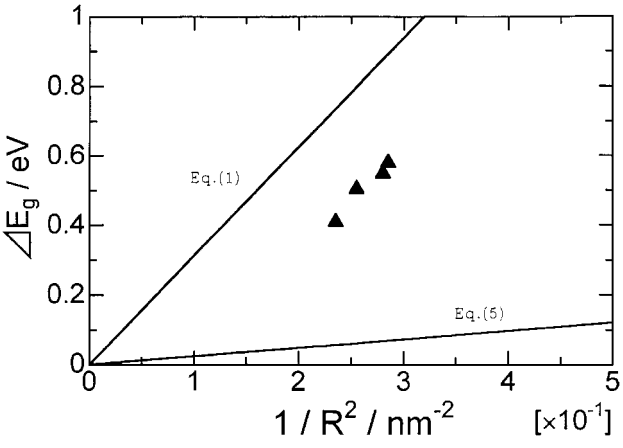

Figure 9 The amount of blue shift, ΔEg, as a function of the square reciprocal radius of the microcrystals for CdSe-doped GeO_2 glass thin films with two theoretical curves of Equation 1 and Equation 5.

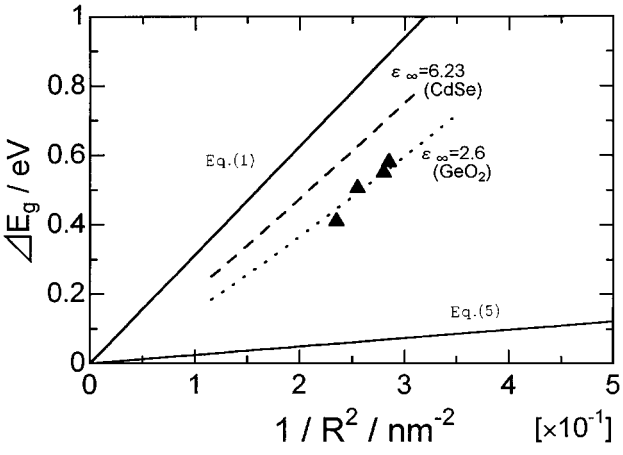

Figure 10 The amount of blue shift as a function of the square reciprocal radius of the mycrocrystals for CdSe-doped GeO_2 glass thin films with the theoretical curves of Equation 3 using ε_∞ of CdSe and GeO_2.

this figure, the experimental relation is successfully explained on the basis of Equation 3 with ε_∞ of GeO_2. This behavior agrees with the results for CdSe-doped SiO_2 glass thin films. In that case, the amount of the blue shift was explained by Equation 3 using ε_∞ of SiO_2. Thus, the influence of the matrix can interprete both case of the quantum size effect.

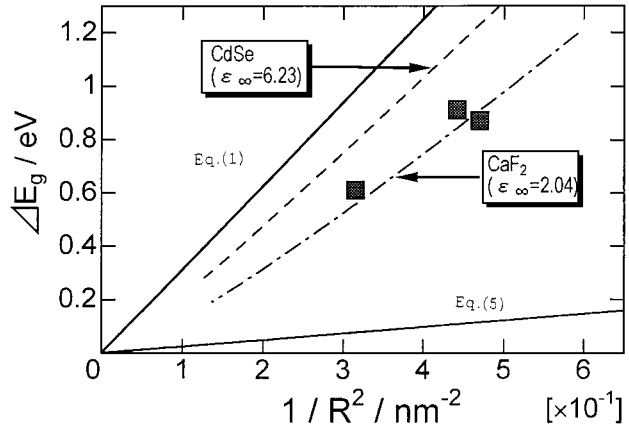

Figure 11 The amount of blue shift as a function of the square reciprocal radius of the microcrystals for CdSe-doped CaF_2 crystal thin films.

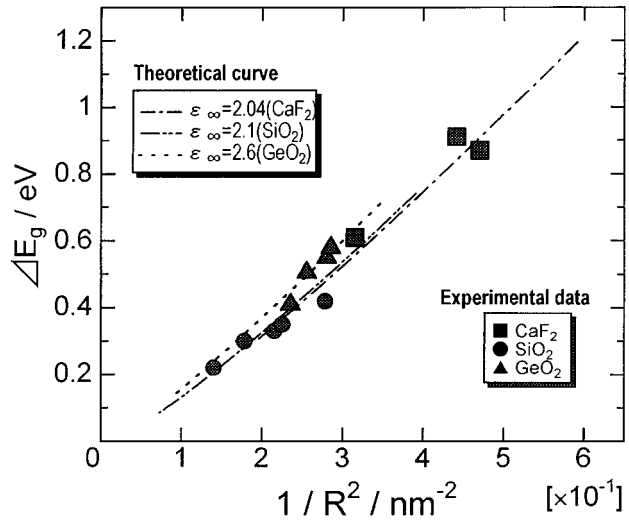

Figure 12 The plot of the amount of blue shift for CdSe-doped SiO_2, GeO_2 and CaF_2 thin films against the square reciprocal radius of the mycrocrystals for CdSe-doped CaF_2 crystal thin films with the theoretical curves of Equation 3 using ε_∞ of the matricies.

Fig. 11 depicts the amount of the blue shift as a function of the microcrystal radius for CdSe-doped CaF_2 film, being based on Equation 3 similarly to the CdSe doped GeO_2 glass thin films. The significant deviation from both theoretical curve of Equations 1 and 5 is also seen. However, by using Equation 3 with ε_∞ of CaF_2, the experimental data is explainable in terms of the quantum size effect which is influenced by the matrix.

The influence of matrix is summarized in Fig. 12. Each point follows the theoretical curve of Equation 3. Three theoretical curves are drawn using ε_∞ of the three different matrix materials. The coincidence among the respective experimental data implies the influence of the matrix. From the results, it is found that the high ε_∞ matrix material gives larger ΔEg and vice versa. In contrast to the dopant with small exciton radius [15], the quantum size effect is clearly influenced by the matrix for the dopant with large exciton radius.

5. Conclusion

CdSe-doped GeO_2 glass and CaF_2 crystal thin films were successfully prepared by magnetron rf-sputtering.

They showed blue shift in optical absorption edge caused by quauntum size effect. The quantum size effect could not explained using simple quantum confinement theories of exciton or electron and hole. The Coulomb interaction and squeezed exciton model must be taken into account, just like CdSe-doped SiO_2 glass films. In specific, the relationship between the amount of the blue shift and the square reciprocal radius depended on the matrix. Therefore, it is concluded that the quantum size effect for the semi-conductor microcrystals with large exciton Bohr radius is strongly influenced by the matrix.

References

1. R. K. JAIN and R. C. LIND, *J. Opt. Soc. Am.* **73** (1983) 647.
2. T. TOKIZAKI, H. AKIYAMA, M. TAKAYA and A. NAKAMURA, *J. Cryst. Growth* **117** (1992) 603.
3. K. HIRAO, S. IIJIMA and H. NASU, *J. Non-Cryst. Solids* **134** (1991) 122.
4. D. C. ROGERS, R. J. MANNING, B. J. AINSLIE, D. COTTER, M. J. YATES, J. M. PARKER and S. MORGAN, *IEEE Photo. Tech. Lett.* **6** (1994) 1017.
5. B. G. POTTER, JR. and J. H. SIMMONS, *J. Appl. Phys.* **68** (1990) 1218.
6. J. A. MEDEIROS NETO, L. C. BARSONA, C. L. CESAR, O. L. ALVES and F. GALEMBECK, *Appl. Phys. Lett.* **59** (1991) 2715.
7. W. SHI, K. LIN and X. LIN, *J. Appl. Phys.* **81** (1997) 2822.
8. M. NOGAMI, Y. W. ZHU and K. NAGASAKA, *J. Non-Cryst. Solids* **134** (1991) 71.
9. H. NASU, J. MATSUOKA and K. KAMIYA, *J. Non-Cryst. Solids* **178** (1994) 148.
10. K. TSUNETOMO, A. KAWABUCHI, H. KITAYAMA, Y. OSAKA and H. NASU, *Jpn. J. Appl. Phys.* **29** (1990) 2481.
11. J. YUMOTO, H. SHIMOJIMA, N. UESUGI, K. TSUNETOMO, H. NASU and Y. OSAKA, *Appl. Phys. Lett.* **57** (1990) 2393.
12. H. NASU, *Brit. Ceram. Trans. and Journal* **89** (1990) 225.
13. H. NASU, S. KANEKO, K. TSUNETOMO and K. KAMIYA, *J. Ceram. Soc. Jpn.* **96** (1991) 266.
14. B. YU, C. ZHU, H. XIA, H. CHEN and F. GAN, *J. Mater. Sci. Lett.* **16** (1997) 2001.
15. H. NASU, T. YAMAMOTO, T. IWANO, T. HASHIMOTO and K. KAMIYA, *J. Ceram. Soc. Jpn.* **106** (1998) 1037.
16. H. HAKEN, *Nuovo Cimento* **10** (1956) 1230.

Received 5 February
and accepted 11 August 1999